A Permeable Vertical Cone Immersed in a Porous Media Saturated with a Nanofluid and Surrounded by a Natural Convection Boundary Layer of a Non-Newtonian Fluid

Shehzad Ali, Dr P. K. Shukla

Mathematics Department of K. G. K. College Moradabad

DOI: https://dx.doi.org/10.51244/IJRSI.2025.1210000236

Received: 23 October 2025; Accepted: 28 October 2025; Published: 15 November 2025

ABSTRACT

A non-Newtonian fluid's free convection boundary-layer flow over a permeable vertical cone embedded in a porous media saturated with a nanofluid was analyzed in order to determine the impact of uniform transpiration velocity. The effects of thermophoresis and Brownian motion are included in the nanofluid model. An effective implicit, iterative, finite-difference method is used to numerically solve the governing partial differential equations once they have been converted into a collection of non-similar equations.

Work that has already been published is compared. In order to demonstrate intriguing aspects of the solutions, a parametric investigation of the physical parameters is carried out, and a typical set of numerical results for the velocity, temperature, and volume fraction profiles as well as the local Nusselt and Sherwood numbers are graphically displayed.

Keywords: Natural convection, thermophoresis, porous medium, non-Newtonian fluid, Nanofluid

INTRODUCTION

In engineering practice, the boundary-layer flow of non-Newtonian fluids in a porous medium with gravity acting as the primary driving factor has drawn a wide range of applications, especially in applied geophysics, geology, ground water flow, and oil reservoir engineering. An adequate understanding of the archeological effects of non-Newtonian fluid flows has become necessary due to the increase in the production of heavy crude oils and other materials whose flow behavior in shear cannot be described by Newtonian relationships. As a result, a new stage in the evolution of fluid dynamic theory is underway.

Similarity solutions for the free convection of non-Newtonian fluids across vertical surfaces in porous media have been proposed by Chen and Chen [1]. The buoyancy-induced flow of non-Newtonian fluids over a nonisothermal horizontal plate immersed in a porous medium has been studied by Mehta and Rao [2]. Yih [3] provides a numerical analysis of the impact of uniform lateral mass flux on natural convection around a cone immersed in a saturated porous material.

Mixed convection–radiation interaction in power-law fluids in a non-isothermal wedge imbedded in a porous medium has been investigated by Mansour and Gorla [4]. Under uniform surface temperature and concentration species, Chamkha and Al-Humoud [5] investigated mixed convection heat and mass transport of non-Newtonian fluids from a permeable surface immersed in a porous media. In an anon-Newtonian fluid, ELHakiem [6] examined how radiation affected non-Darcy natural convection over a vertical heated surface in a saturated porous medium with mass transfer. In the presence of internal heat generation and absorption, Datti and Prasad [7] provided a numerical solution for heat transfer in the flow of a non-Newtonian power-law fluid across a non-isothermal stretched sheet while submerged in a saturated porous media.

ISSN No. 2321-2705 | DOI: 10.51244/IJRSI | Volume XII Issue X October 2025

When considering a non-Newtonian power-law fluid flow over a permeable wedge embedded in a fluidsaturated porous media, Chamkha [8] examined coupled heat and mass transport by mixed convection. .

Nomenclature:

C : Nano particle volume fraction

C_w: Nano particle volume fraction at the surface of the cone

C_∞: Ambient nanoparticle volume fraction attained as y tends to infinity

D_B: Brownian diffusion ncoefficient DT: Thermophoretic diffusion coefficient f $_D$: dimensionless stream function g : Gravitational acceleration vector

K : Permeability of porous medium

K_m: Thermal conductivity

Le: Lewi snumber

Nr: Buoyancy Ratio

Nb: Brownian motion parameter

Nt: Thermophoresis parameter

N: Power-law index

Nu_x: Local Nusselt number

Ra_x: Local Rayleigh number

Sh_x: Local Sherwood number

T: Temperature

T_w: Temperature at vertical plate

$T_{\infty:}$ Ambient temperature attained as y tends to infinity u, v: Velocity components

$V_{w:}$ Uniform transpiration velocity

(Xiyu) : Cartesian coordinates Greek symbols α: Thermal diffusivity of porous medium β: Volumetric expansion coefficient of fluid γ: Half angle of thecone μ: Fluid viscosity η, ξ: Similarity *and non*-similarity parameters θ : Dimensionless temperature φ: Dimensionless nanoparticle volume fraction ψ: Stream function ρ_f: Fluid density ρ_p : nanoparticle mass density

$(\rho c)_f$: Heat capacity of the fluid

$(\rho c)_p$: Effective heat capacity of nanoparticle material τ : Parameter defined by Eq.(3)

Subscripts

ISSN No. 2321-2705 | DOI: 10.51244/IJRSI | Volume XII Issue X October 2025

W : Conditions at the wall

∞: Conditions in the free stream.

It is well known, however, that traditional heat transfer fluids, such as water, oil, and ethylene eglycol mixture, are poor heat transfer fluids because their thermal conductivity has a significant impact on the coefficient of heat transfer between the heat transfer surface and the heat transfer medium. Over the past few years, a novel method for enhancing heat transmission by introducing ultra-fine solid particles into fluids has been widely applied. Choi [9] coined the term "nanofluid" to describe these fluids that suspend nanoscale particles in the base fluid.

According to Choi et al. [10], adding nanoparticles to conventional heat transfer liquids in modest amounts (less than 1% by volume) boosted the fluid's thermal conductivity by up to about two times. Thermal conductivity augmentation is a property of nanofluids, as noted by Masuda et al. [11]. The potential application of nanofluids in sophisticated nuclear systems is suggested by these phenomena [12]. It appears that Khanafer et al. [13] are the first to have investigated the heat transfer performance of nanofluids within an enclosure while accounting for the dispersion of solid particles. Buongiorno conducted a thorough investigation of convective transport in nanofluids [14].

Oztop and Abu-Nada [15] used nanofluids containing different kinds of nanoparticles to investigate heat transmission and fluid flow caused by buoyant forces in a partially heated enclosure. They discovered that using nanofluids improved heat transfer, and that this improvement is more noticeable at low aspect ratios than at high ones. Natural convection past a vertical plate in a porous media saturated with a nanofluid has been investigated by Nield and Kuznetsov [16]. The effects of thermophoresis and Brownian motion are included in the nanofluid model. The classical problem of free convection boundary layer flow of a viscous and incompressible fluid (Newtonian fluid) past a vertical flat plate has also been explored by Kuznetsov and Nield [17] in the context of nanofluids.

Using several kinds of nanoparticles, Syakila and Pop [18] investigated the constant mixed convection boundary layer flow via a vertical flat plate embedded in a porous medium full of nanofluids. The natural convection past a sphere embedded in a porous media saturated by a nanofluid has also been examined recently by Chamkha et al. [19].The constant boundary layer flow of a nanofluid on a stretching circular cylinder in a stagnant free stream was investigated by Gorla et al. [20]. The mixed convection past a vertical wedge embedded in a porous medium saturated by a nanofluid was examined by Gorla et al. [21].

In the presence of heat generation or absorption effects, Chamkha et al. [22] investigated the laminar MHD mixed convection flow of a nanofluid along a stretched permeable surface. The impact of radiation on mixed convection over a wedge embedded in a porous media containing a nanofluid was examined by Chamkha et al. [23]. The natural convection from a vertical permeable cone in nanofluid-saturated porous media for homogeneous heat and nanoparticle volume fraction fluxes was investigated by Chamkha and Rashad [24]. This study's goal is to examine how a non-Newtonian fluid's free convection boundary layer flow over a permeable vertical cone embedded in a porous media saturated with a nanofluid is affected by uniform transpiration velocity.

For the nanofluid, the effects of thermophoresis and Brownian motion are considered. For a range of values of the nanofluid parameters governing the problem, numerical solutions of the boundary layer equations are derived and discussed.It has been discussed how velocity, temperature, and the volume fraction profiles of nanoparticles, along with the local Sherwood and Nusselt numbers, depend on these parameters.

Governing equations:

Examine how a non-Newtonian fluid flows across a permeable vertical cone embedded in a porous media saturated with a nanofluid via free convection boundary-layer flow when the transpiration velocity is uniform. Brownian motion and thermophoresis effects are included in the nanofluid model. It was assumed that the ambient temperature and the volume fraction of nanoparticles distant from the cone's surface, T_∞ and C_∞, were

uniform, and that the cone surface was kept at a constant temperature (T_w) and nanoparticle volume fraction (C_w).

For $T_w > T_\infty$ and $C_w > C_\infty$ an upward flow is induced as a result of the thermal and nanoparticle volume fraction buoyancy effects. The flow model and physical coordinate system are displayed in Fig. 1. Where x and y are Cartesian coordinates that measure distance along and normal to the cone's surface, respectively, the origin of the coordinate system is positioned at the cone's vertex. We use the non-Newtonian power-law fluid flow model in a porous media that was put forth by Dharmadhikari and Kale [26] and Christopher and Middleman [25]. With the boundary layer, Boussinesq approximations, and the modified Darcy rule, the governing equations for the problem under discussion can be expressed as

(see [3]):

$$\frac{\partial(ru)}{\partial x} + \frac{\partial(rv)}{\partial v} = 0, \qquad (1)$$

$$\frac{\partial u^n}{\partial y} = \frac{(1 - C_\infty)\rho f_\infty \cos\gamma \beta g K}{\mu}\frac{\partial T}{\partial y} - \frac{(\rho_p - \rho f_\infty)\cos\gamma g K}{\mu}\frac{\partial C}{\partial y}, \qquad (2)$$

$$u\frac{\partial T}{\partial x} + v\frac{\partial T}{\partial y} = \alpha\frac{\partial^2 T}{\partial y^2} + \tau\left[D_B \frac{\partial C}{\partial y}\frac{\partial T}{\partial y} + (T_\infty)\left(\frac{\partial T}{\partial y}\right)^2\right] \qquad (3)$$

$$u\frac{\partial C}{\partial x} + v\frac{\partial C}{\partial y} = D_B\frac{\partial^2 C}{\partial y^2} + \left(\frac{D_T}{T_\infty}\right)\frac{\partial^2 T}{\partial y^2}, \qquad (4)$$

where the vertical and horizontal directions are indicated by the letters x and y, respectively. The x- and y components of velocity, temperature, and nanoparticle volume fraction are denoted by the letters u, v, T, and C, respectively. The coefficients of permeability, volumetric expansion of fluid, gravitational acceleration vector, Brownian diffusion coefficient, and thermophoretic diffusion coefficient are denoted as K, β, g, D_B, and D_T, respectively.

γ, μ, ρ_f and ρ_p are the half angle of the cone, fluid viscosity, fluid density and nanoparticle mass density, respectively. $\alpha = k_m/(\rho c)_f$ and $\tau = (\rho c)_p/(\rho c)_f$ are the thermal diffusivity of porous medium and the ratio of heat capacities, respectively. k_m, $(\rho c)_f$ and $(\rho c)_p$ are thermal conductivity, heat capacity of the fluid and the effective heat capacity of the nanoparticle material, respectively. We note that $n < 1$ and >1 represent pseudoplastic fluid and dilatant fluid, respectively.

The boundary conditions suggested by the physics of the problem are given by

$$y = 0: \quad v = V_w,\ T = T_w,\ C = C_w, \qquad (5a)$$

$$y \to \infty: \quad u = 0,\ T = T_\infty,\ C = C_\infty \qquad (5b)$$

where V_w, T_∞ and C_∞ are the uniform transpiration velocity, temperature and nanoparticle volume fraction, respectively. We made the assumption that the boundary layer was suitably thin in relation to the cone's local radius. The proximity of a local

ISSN No. 2321-2705 | DOI: 10.51244/IJRSI | Volume XII Issue X October 2025

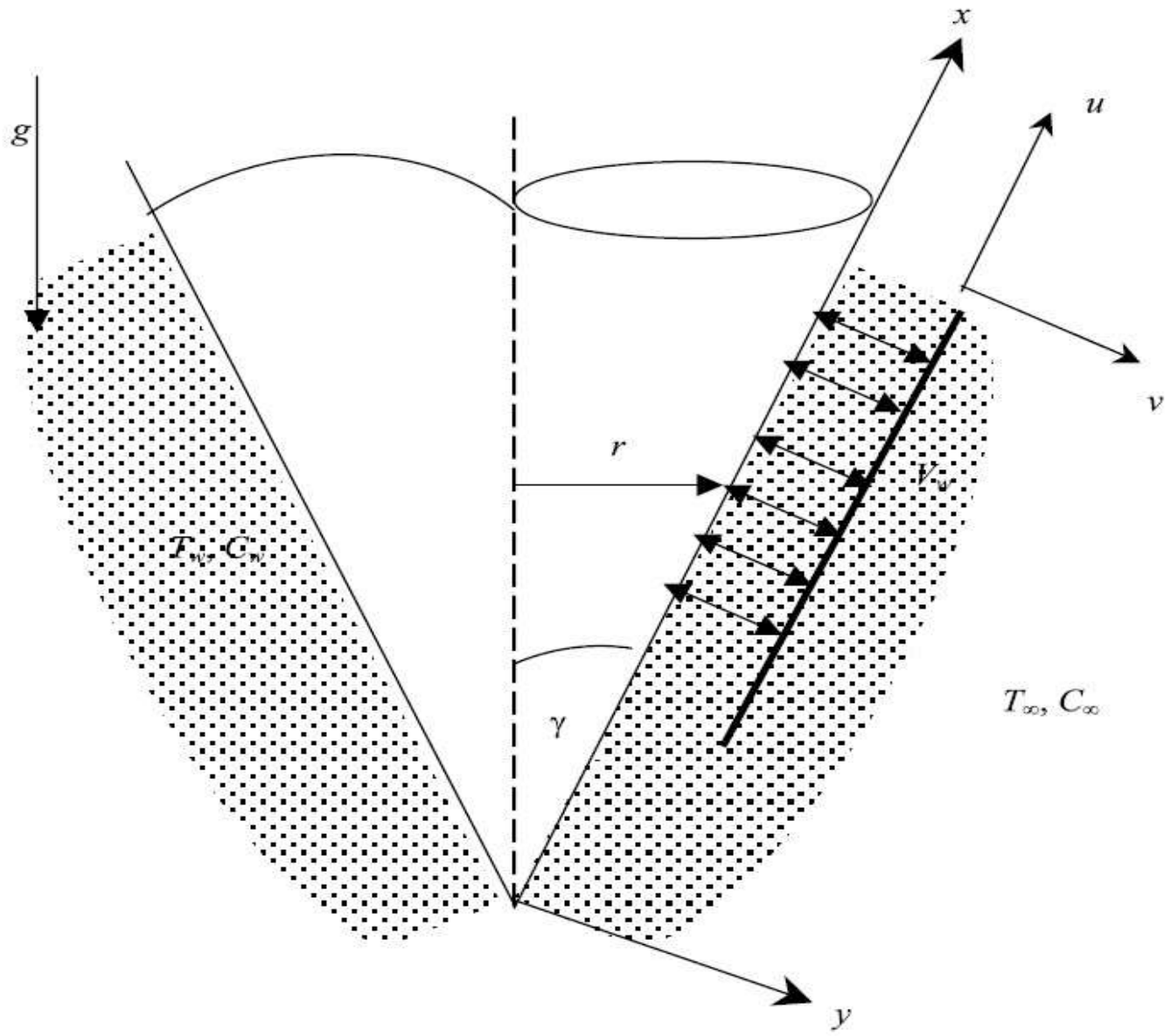

Fig. 1. The physical coordinate system and flow model

point in the boundary layer, therefore, can be replaced by the radius of the cone r, i.e., r = x sin γ, invoking the following dimensionless variables. This can be done by introducing the stream function such that:

ru = $\partial\psi/\partial y$, rv = $-\partial\psi/\partial x$ and using

$$\xi = \frac{2V_w x}{}^{1/2}, \eta = x\overline{R}a_x^{\ 1/2}, f(\xi,\eta) = \alpha r R\_\_\_\_\_ a_{x1/2}, \theta(\xi,\eta) = (\_\_\_\_\_ T_w - T_\infty), \alpha Ra_x$$

$$\phi^{(\xi,\eta)} = \frac{(C - C_\infty)}{(C_w - C_\infty)}. \qquad (6)$$

Substituting Eq. (6) into Eqs. (1)–(4) produces the following non-similar equations:

$$nf'^{n-1}f'' = \theta' - N_r\phi', \qquad (7)$$

$$\theta'' + N_b\phi'\theta' + \ - \ 3\, f\theta' + N_t\theta'^2 = 1\,\xi\,(\cancel{f'\partial\theta} - \cancel{\theta'\partial f}), \qquad (8)$$

ISSN No. 2321-2705 | DOI: 10.51244/IJRSI | Volume XII Issue X October 2025

$$\phi'' + \frac{3Le}{2} f\phi' + \frac{N_b}{N_t}\theta'' = \frac{Le}{2}\xi\left(f'\frac{\partial\phi}{\partial\xi} - \phi'\frac{\partial f}{\partial\xi}\right), \quad (9)$$

$$\eta = 0: \quad f = -\frac{\xi}{4}, \quad \theta = 1, \ \phi = 1, \quad (10a)$$

$$\eta \to \infty: \quad \theta = 0, \phi = 0, \quad (10b)$$

where $N_r = \frac{(\rho_P - \rho f_\infty)(C_w - C_\infty)}{\rho f_w \beta (T - T_\infty)(1 - C_\infty)}$, $N_b = \frac{(\rho c)_p D_B (C_w - C_\infty)}{(\rho c) f \alpha}$, $N_t = \frac{(\rho c)_p T_B (T_w - T_\infty)}{(\rho c) f \alpha T_\infty}$

$$Le = \alpha / D_B, \quad Ra_x = (x/\alpha)\{(1 - C_\infty)\rho f_\infty g \cos\gamma \beta K (T_w - T_\infty)/\mu\}^{\frac{i}{n}} \quad (11)$$

are the buoyancy ratio, Brownian motion parameter, thermophoresis parameter, Lewis number, and modified local Rayleigh number, respectively. It should be noted that the mass flux parameter $\xi = 0 (V_w = 0)$ corresponds to impermeable cone surface while $\xi > 0 (V_w > 0)$ corresponds to the case of fluid injection and $\xi < 0 (V_w < 0)$ corresponds to the case of fluid injection. Of special significance for this problem are the local Nusselt and Sherwood numbers. These physical quantities can be defined as:

$$Nu_x Ra_x^{-1/2} = -\theta'(\xi, 0), \quad (12)$$

$$Sh_x Ra_x^{-1/2} = -\phi'(\xi, 0). \quad (13)$$

Table-1

Values of $-\theta'(\xi, 0)$ for various values of n in the absence of nanoparticle volume fraction, Brownian motion and thermosphoresis effects ($N_r = N_b = N_t = 0$).

n	Yih [3]	Present results
0.5	0.6522	0.65225
0.8	0.7339	0.73394
1.0	0.7686	0.76865
1.5	0.8233	0.82336
2.0	0.8552	0.85524

Numerical method and validation:

Since they are nonlinear and lack an analytical solution, the non-similar Eqs. (7)–(9) require numerical solutions. For the solution of such equations, Blottner's [27] effective, iterative, tri-diagonal, implicit finitedifference technique has been shown to be sufficient. After linearizing the equations, they are discretized using two-point backward difference formulas in the η direction with a constant step size and three-point central difference quotients in the η direction with varying step sizes. The resulting equations can be solved using the well-known Thomas algorithm (see [27]) and create a tri-diagonal system of algebraic equations. After solving Eqs. (10)–

(12) at $\xi = 0$, the solution process proceeds by applying the solution to the previous line of constant ξ until it reaches the target value of ξ.

An iterative solution using consecutive over or under relaxation techniques is necessary because of the equations' nonlinearities. The largest absolute error between two consecutive iterations must be 10^{-6} in order to satisfy the convergence requirement. There were 196 grids in the η direction and 101 grids in the ξ direction that comprised the computational domain. Very accurate results were obtained with a constant step size of 0.01 in the ξ direction and a starting step size of 0.001 in the η direction with an increase of 1.035 times the previous step size.

It was expected that the ambient conditions were represented by $\eta(\eta_\infty)$, with a maximum value of 35. After conducting numerical experiments to evaluate grid independence and guarantee the accuracy of the results, the step sizes used were determined. Direct comparisons with the numerical results previously reported by Yih [3]—different values of n and ξ in the absence of the nanoparticle volume fraction, Brownian motion, and thermophoresis effects ($Nr = N_b = Nt = 0$)—validated the accuracy of the previously indicated numerical method. Table 1 displays this comparison. This table shows that there is excellent agreement between the outcomes. This positive contrast gives the numerical results that will be presented in the following section more credibility.

RESULTS AND DISCUSSION

In this section, a representative set of graphical results for the dimensionless velocity $f'(\xi, \eta)$, temperature $\theta(\xi, \eta)$, and nanoparticle volume fraction $\phi(\xi, \eta)$ as well as the local Nusselt number $Nu_x Ra_x^{-1/2} = -\theta'(\xi, 0)$ (reciprocal of rate of heat transfer), and the local Sherwood number $Sh_x Ra_x^{-1/2} = -\phi'(\xi, 0)$ (reciprocal of rate of volume fraction transfer) is presented and discussed for various parametric conditions. These conditions are intended for various values of and the viscosity index n, the buoyancy ratio N_r, Brownian motion parameter N_b, thermophoresis parameter N_t and Lewis number Le, respectively.

Fig. 2(a)–(c) present the effect of viscosity index n on the velocity f', temperature θ and nanoparticle volume fraction ϕ, respectively. It can be seen that the velocity profile for shear-thickening or dilatant fluids ($1 < n < 2$) is larger than that for shear-thinning or pseudo-plastic fluids ($0 < n < 1$), it can be seen that both the temperature θ and nanoparticle volume fraction ϕ of the fluid decrease as viscosity index n increases, while the velocity f' increases as viscosity index n increases. On the other hand, Figs. 3 and 4 show the influence of viscosity index n on the local Nusselt number $-\theta'(\xi, 0)$ and the local Sherwood number $-\phi'(\xi, 0)$, respectively. From these figures, it is observed that the power-law fluid viscosity indices n = 0.8, 0.9 (shear-thinning or pseudo-plastic fluid), n = 1.0 (Newtonian fluid) and n = 1.1, 1.2 (shear-thickening or dilatant fluid), respectively. However, as the values of viscosity index n increased it led to an increase in both the local Nusselt and Sherwood numbers.

Fig. 5(a)–(c) present the effect of the buoyancy ratio N_r on the velocity f', temperature θ and nanoparticle volume fraction ϕ, respectively. It can be seen that the increases of the value of the buoyancy ratio N_r has a tendency to the fluid motion along the cone surface which filled with nanofluids. This behavior in the flow velocity is accompanied by slight increases in the fluid temperature and volume fraction as N_r increases from 0.1 to 0.7. On the other hand, Figs. 6 and 7 show the influence of the buoyancy ratio N_r on the local Nusselt number $-\theta'(\xi, 0)$ and the local Sherwood number $-\phi'(\xi, 0)$, respectively. The increases in the fluid temperature and volume fraction profiles as Nr increases mentioned above causes the values of the wall temperature and volume fraction slopes to enhance yielding reductions in both the local Nusselt and Sherwood numbers.

Fig. 8(a)–(c) display the effect of increasing the Brownian motion parameter N_b from 0.1 to 0.7 on the velocity, temperature and volume fraction profiles, respectively. It can be observed that the increasing the value of the Brownian motion parameter N_b causes increases in both the velocity and temperature profiles with a significant decrease on the volume fraction profiles. These behaviours are clearly shown in Fig. 8(a)–(c).

ISSN No. 2321-2705 | DOI: 10.51244/IJRSI | Volume XII Issue X October 2025

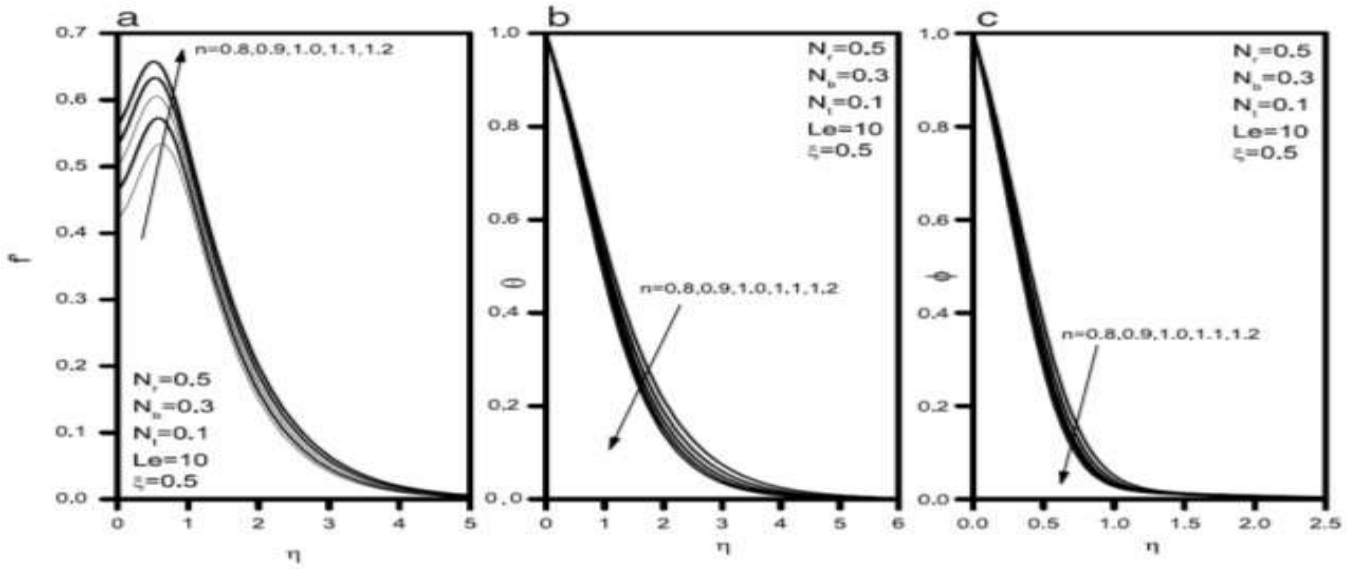

Fig. 2 Effect of n on the (a) velocity, (b) temperature, (c) volume fraction profiles.

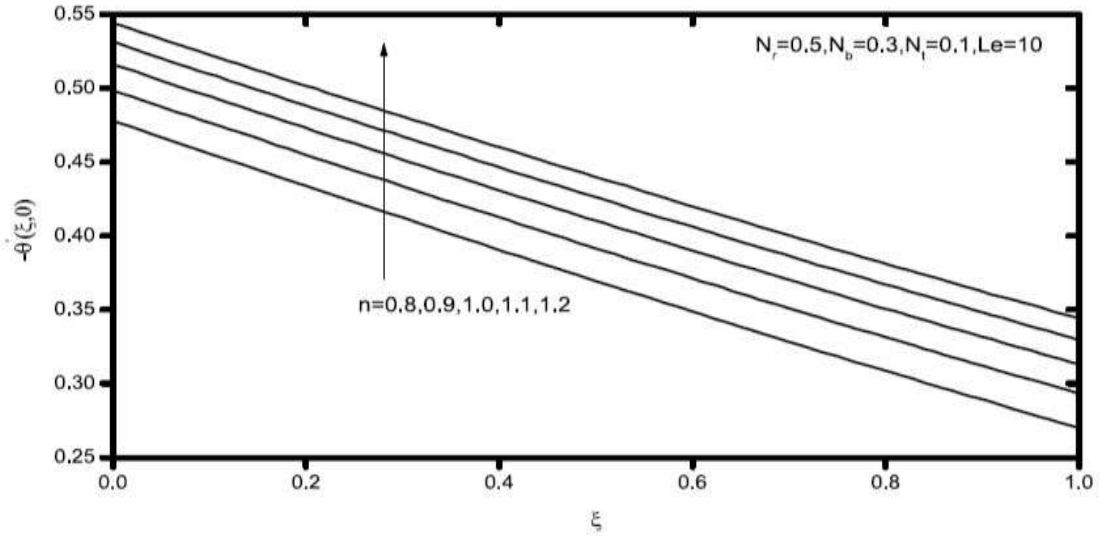

Fig. 3 The local Nusselt number is affected by n.

.

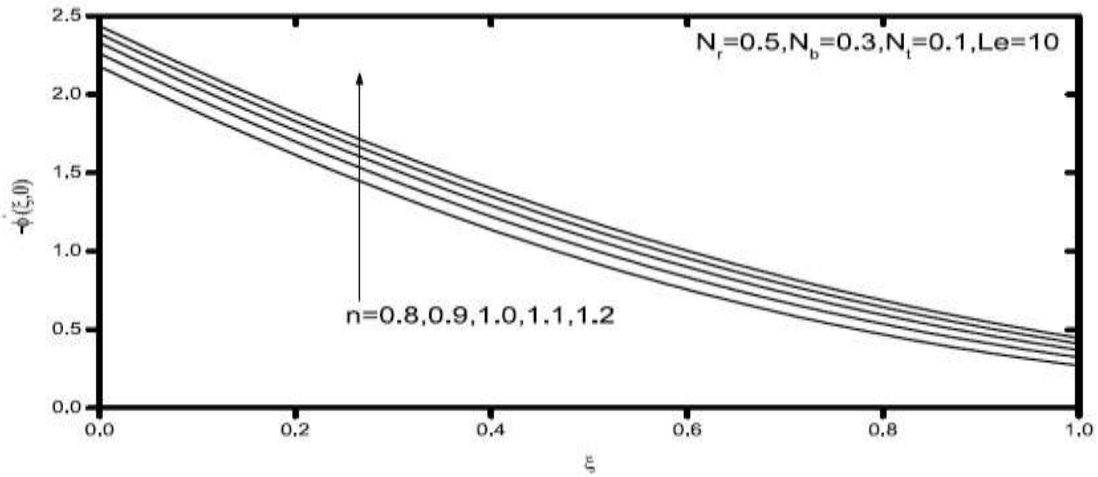

Fig. 4. Effect of n on the local Sherwood number.

ISSN No. 2321-2705 | DOI: 10.51244/IJRSI | Volume XII Issue X October 2025

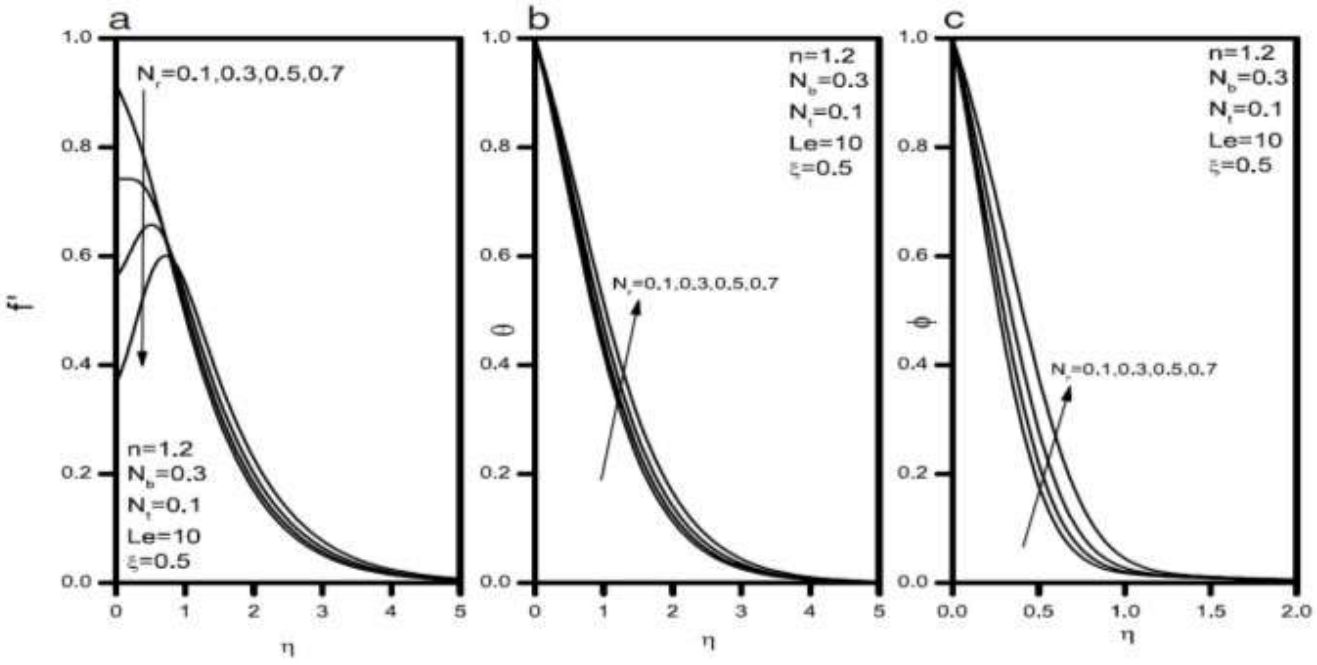

Fig. 5. Effect of N_r on the (a) velocity, (b) temperature, (c) volume fraction profiles.

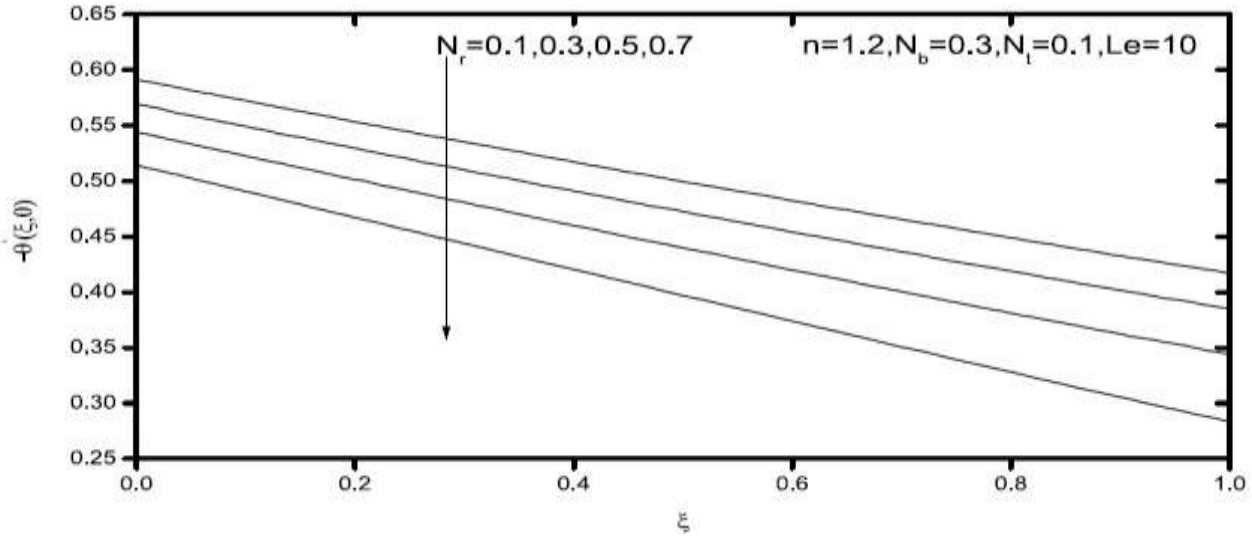

Fig. 6. Effect of N_r on the local Nusselt number.

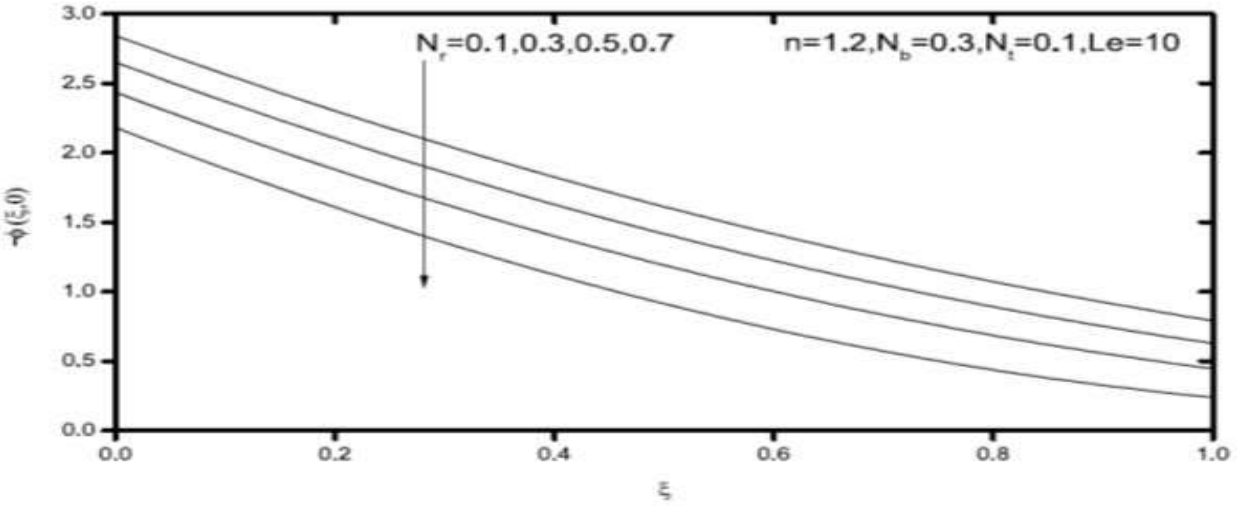

Fig. 7. Effect of N_r on the local Sherwood number.

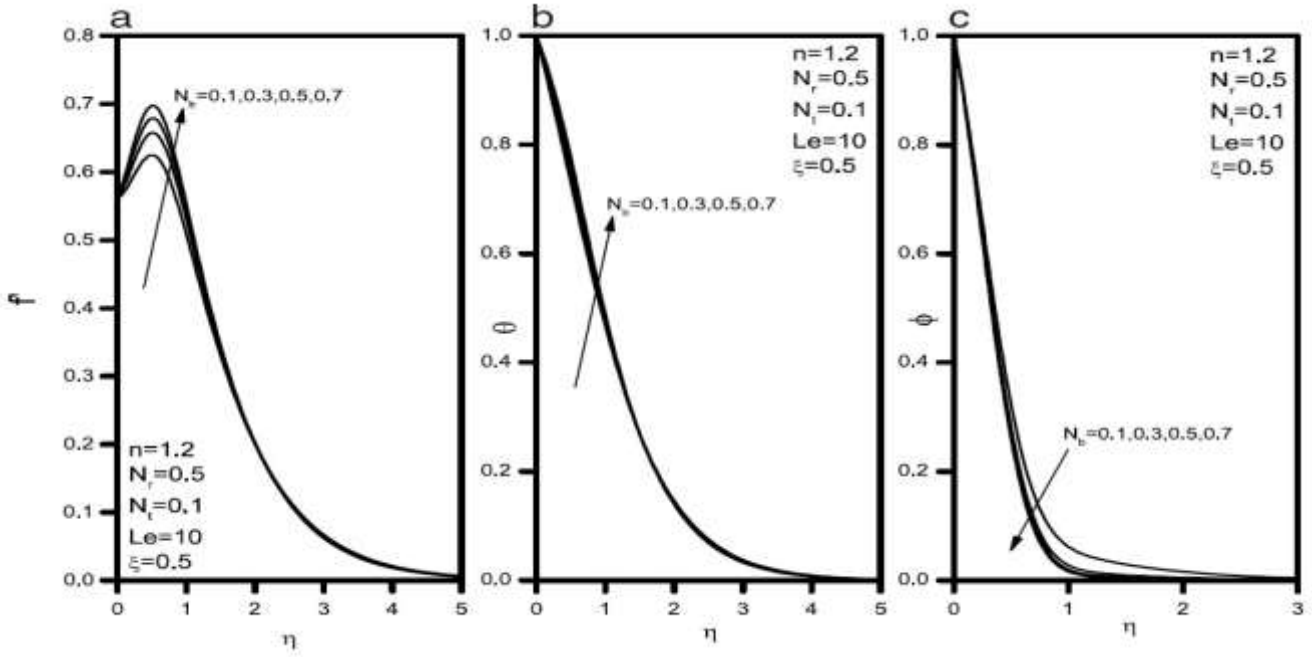

Fig. 8. Effect of N_b on the (a) velocity, (b) temperature, (c) volume fraction profiles.

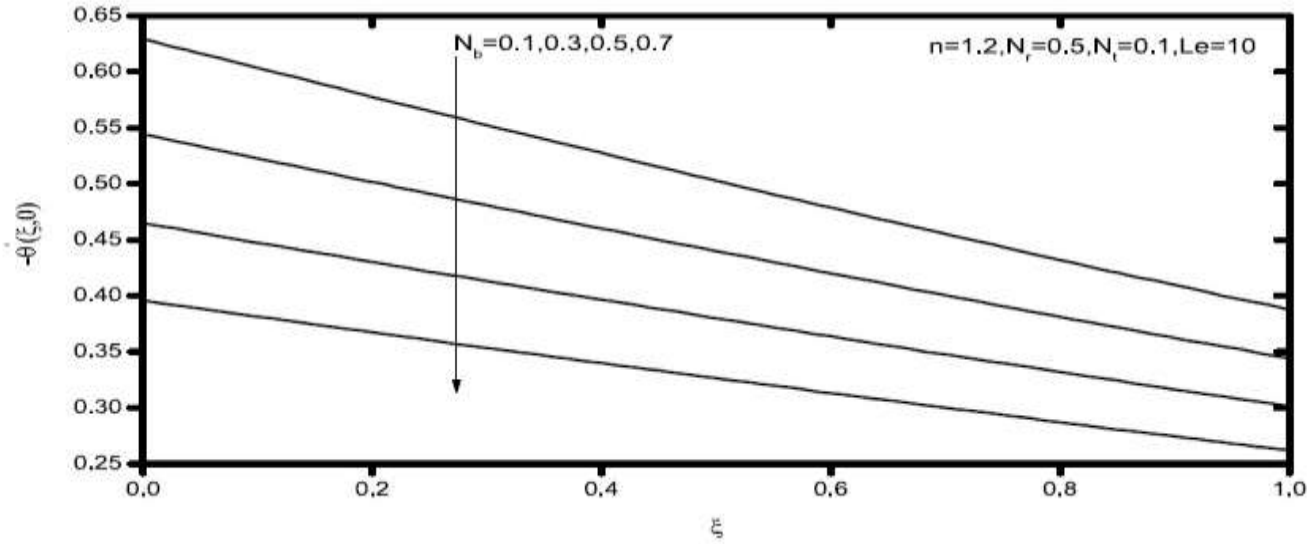

Fig. 9. Effect of N_b on the local Nusselt number.

Figs. 9 and 10 illustrate the effect of the Brownian motion parameter Nb on the local Nusselt number $-\theta'(\xi, 0)$ and local Sherwood number $-\phi'(\xi, 0)$, respectively. As indicated before, increasing the Brownian motion parameter N_b causes increasing in the temperature profiles while its volume fraction decreases. This yields reduction in the local Nusselt number and enhancement in the local Sherwood number.

Fig. 11(a)–(c) present the velocity, temperature and nanoparticle volume fraction profiles for various values of thermophoresis parameter N_t, respectively. Increases in the thermophoresis parameter N_t have the tendency to increase the velocity profiles as well as the fluid temperature and volume fraction profiles. Figs. 12 and 13 display the effect of the thermophoresis parameter N_t on the values of $-\theta'(\xi, 0)$ and $-\phi'(\xi, 0)$, respectively. Increasing the value of the thermophoresis parameter N_t results in increasing both the temperature and volume fraction profiles causing the values of $-\theta'(\xi, 0)$ and $-\phi'(\xi, 0)$ to decrease, respectively as N_t increases.

Fig. 14(a)–(c) show the representative temperature and nanoparticle volume fraction profiles for different values of Lewis number Le, respectively. It is clearly noted that the velocity increases while both the fluid temperature and volume fraction as well as its boundary-layer thickness decrease considerably as the Lewis number Le increases.

ISSN No. 2321-2705 | DOI: 10.51244/IJRSI | Volume XII Issue X October 2025

Finally, Figs. 15 and 16 present the effects of the Lewis number Le on the local Nusselt number $-\theta'(\xi, 0)$ and local Sherwood number $-\phi'(\xi, 0)$, respectively. As mentioned before, increasing the Lewis number Le causes enhancements in both the heat and mass transfer effects represented by increases in the local Nusselt and Sherwood numbers.

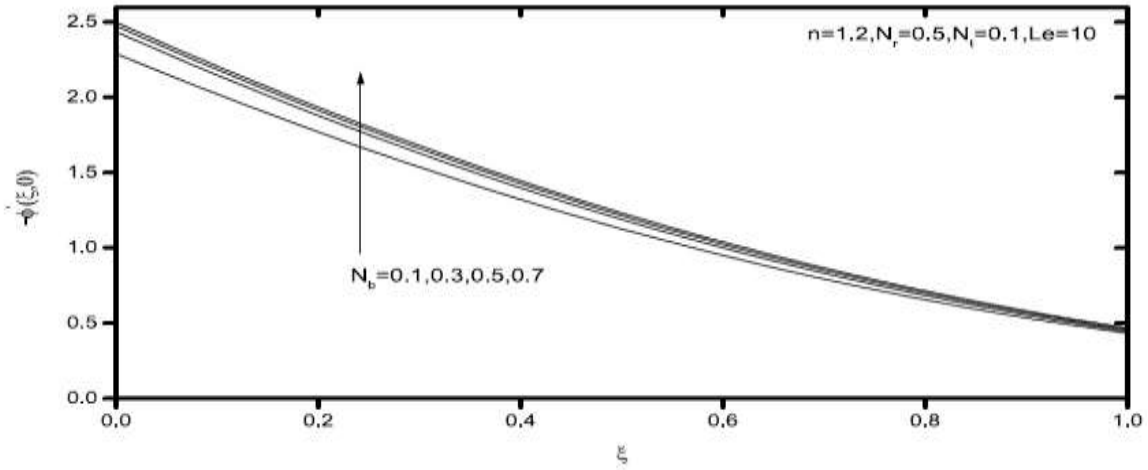

Fig. 10. Effect of N_b on the local Sherwood number.

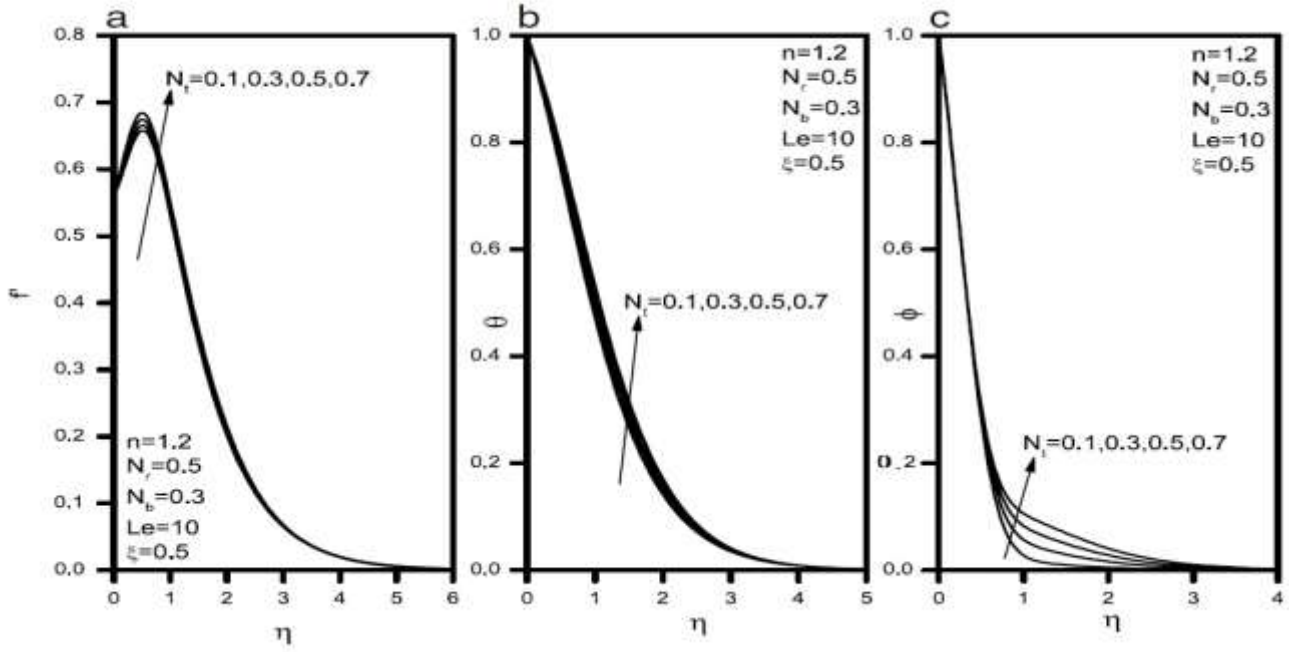

Fig. 11. Effect of N_t on the (a) velocity, (b) temperature, (c) volume fraction profiles.

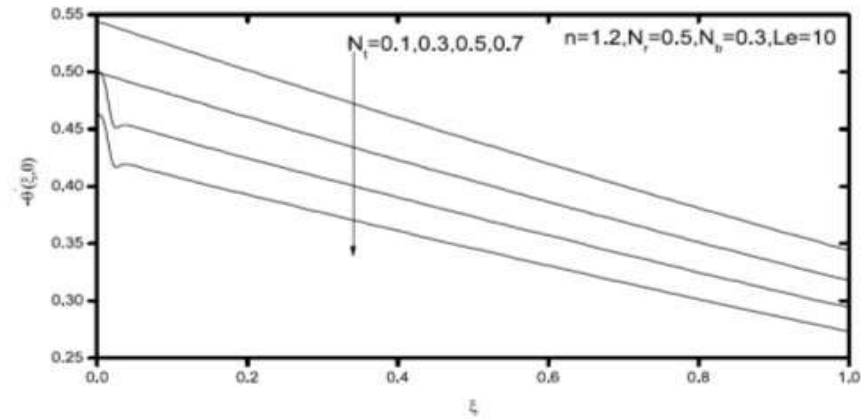

Fig. 12. Effect of N_t on the local Nusselt number.

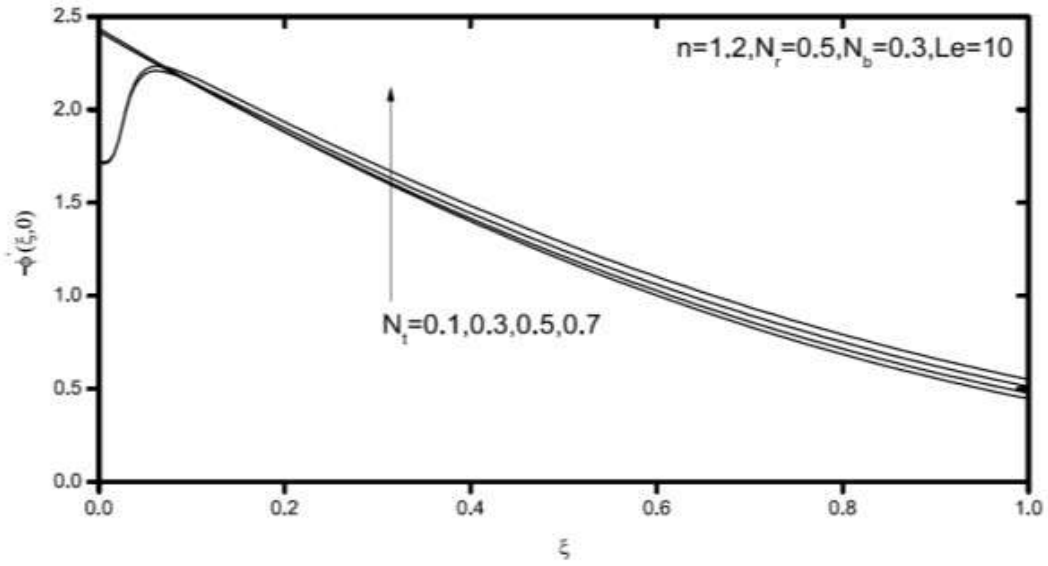

Fig. 13. Effect of N_t on the local Sherwood number.

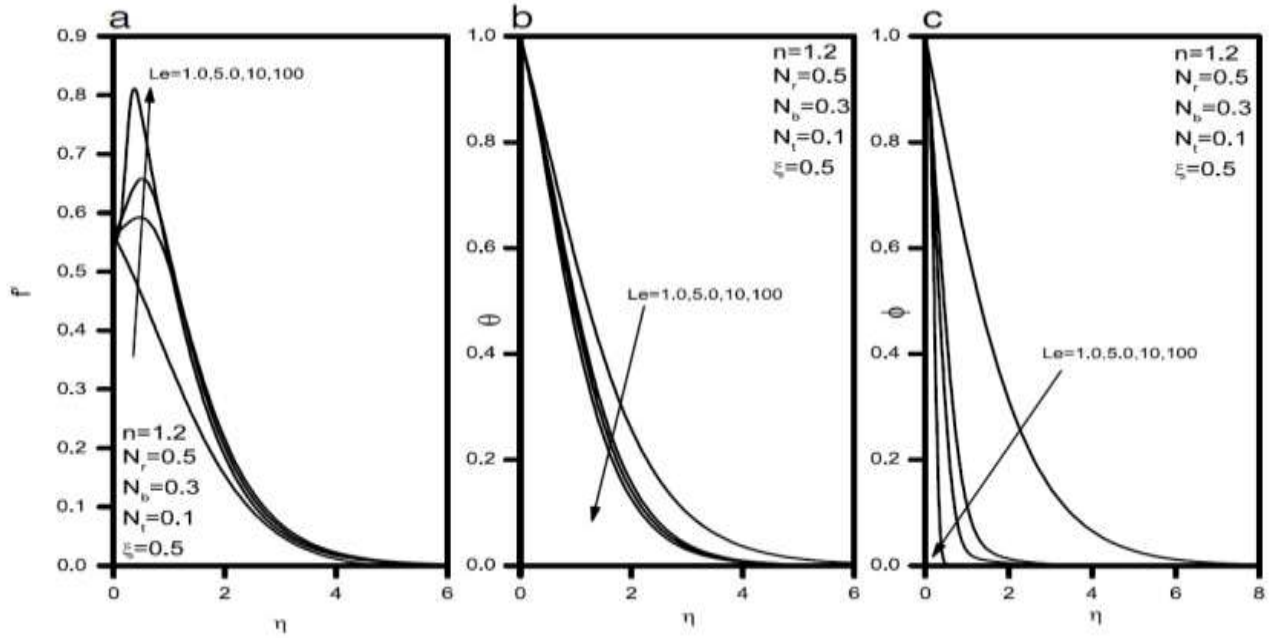

Fig. 14. Effect of Le on the (a) velocity, (b) temperature, (c) volume fraction profiles.

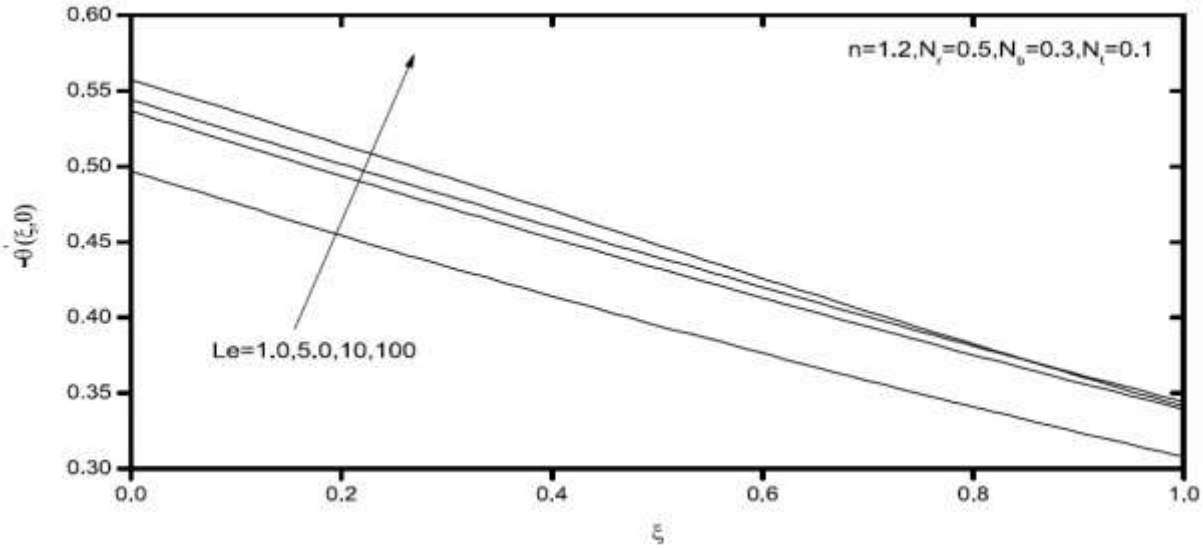

Fig. 15. Effect of Le on the local Nusselt number.

ISSN No. 2321-2705 | DOI: 10.51244/IJRSI | Volume XII Issue X October 2025

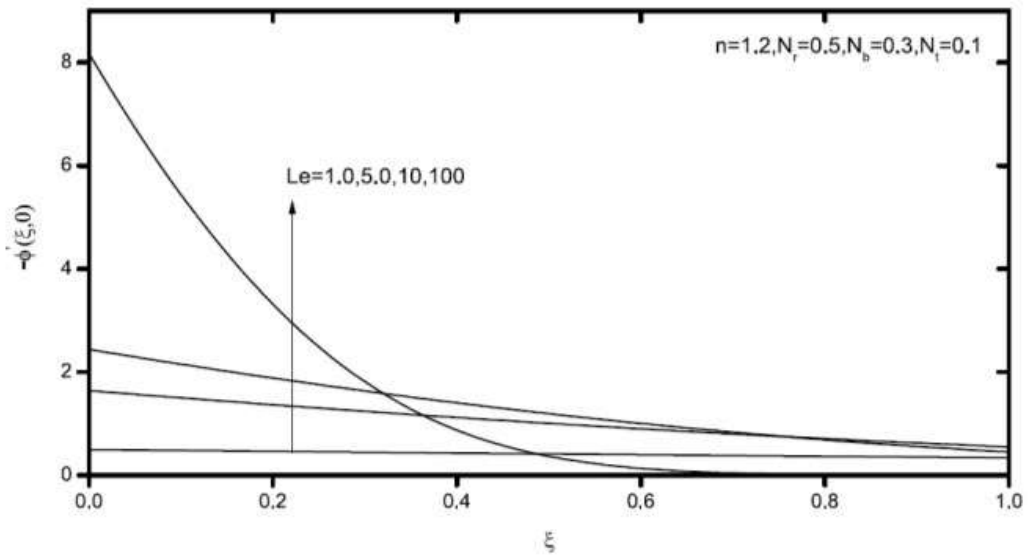

Fig. 16. Effect of Le on the local Sherwood number.

CONCLUSIONS

The topic of uniform transpiration velocity on free convection boundary-layer flow of a nonNewtonian fluid over a permeable vertical cone embedded in a porous media saturated with a nanofluid has been theoretically investigated in the current work. The effects of thermophoresis and Brownian motion are included in the nanofluid model. An effective implicit finited-ifference method was used to solve the resulting non-similar differential equations numerically. The findings concentrated on how the local Nusselt and Sherwood numbers were impacted by the buoyancy ratio, Lewis number, thermophoresis parameter, and Brownian motion parameter.

It was discovered that both the local Sherwood and Nusselt numbers increased when the viscosity index values increased. However, the local Sherwood and Nusselt values declined as the buoyancy ratio increased.Furthermore, it was determined that the local Sherwood number grew and the local Nusselt number fell as the Brownian motion parameter increased. But they do.Additionally, raising the Lewis number led to increases in the local Sherwood and Nusselt numbers.In order to improve heat transfer in a porous medium as efficiently as possible, future research may be necessary to determine the ideal value of the solid volume fraction parameter of non-Newtonian nanofluids. However, this is outside the purview of this study.

In light of this, it is important to note that research on non-Newtonian nanofluids is still in its infancy and that it appears to be very challenging to accurately understand how the use of nanoparticles behaves in convective flow in porous media. Complementary work is required to comprehend the heat transfer properties of nonNewtonian nanofluids and find new uses for them.

In light of this, it is important to note that research on non-Newtonian nanofluids is still in its infancy and that it appears to be very challenging to accurately understand how the use of nanoparticles behaves in convective flow in porous media. Complementary work is required to comprehend the heat transfer properties of nonNewtonian nanofluids and find new uses for them.

REFERENCES

1. H.T.Chen,C.K.Chen,Free convection of non Newtonian fluids along a vertical plate embedded in a porous medium,Trans.ASME, J. Heat Transfer 110 (1988) 257–260.
2. K.N.Mehta,K.N. Rao,Buoyancy-induced flow of non-Newtonian fluids over a non-isothermal horizontal plate embedded in a porous medium, Internat. J.Engrg.Sci.32 (1994) 521–525.
3. K.A. Yih, uniform latera lmass flux effect on natural convection of non-Newtonian fluids over a cone in porous media, Int.Commun. Heat MassTransfer 25 (7) (1998) 959–968.

4. M.A. Mansour, R.S.R. Gorla, Mixed convection–radiation interaction in power-law fluids along a nonisothermal wedge embeddedin a porous medium, Transp.Porous Media30 (1998) 113–124.
5. A.J. Chamkha, J. Al-Humoud, Mixed convection heat and mass transfer of non-Newtonian fluids from a permeable surface embedded in a porous medium,Int.J.Numer.Methods Heat Fluid Flow17 (2007) 195–212.
6. M.A. EL-Hakiem, Radiative effects on non-Darcy natural convection from a heated vertical plate in saturated porous media with mass transfer for non-Newtonian fluid, J. Porous Media 12 (2008) 89–99.
7. P.S. Datti, K.V. Prasad, Non-Newtonian power law fluid flow and heat transfer in a porous medium over a non-isothermal stretchings heet, Int.J. Fluid Mech.Res.35 (2008) 417–433.
8. Ali J. Chamkha,Heat and mass transfer of a non-Newtonian fluid concentration and heat source or sink,WSEAS Trans.Heat MassTrans.1(5) (2010) 11–20.
9. S.U.S. Choi, Enhancing thermal conductivity of fluids with nanoparticle, in: D.A. Siginer, H.P. Wang (Eds.), Developments and Applications of Non-Newtonian Flows, ASME FED, vol.231/MD, vol. 66,1995, pp. 99–105.
10. S.U.S. Choi, Z.G. Zhang, W.Yu, F.E. Lockwood, E.A. Grulke, Anomalously thermal conductivity enhancement in nano tube suspensions,Appl.Phys.Lett. 79 (2001) 2252–2254.
11. H. Masuda, A. Ebata, K. Teramae, N. Hishinuma, Alteration of thermal conductivity and viscosity of liquid by dispersing ultra-fine particles, Netsu Bussei7(1993)227–233.
12. J. Buongiorno, W. Hu , Nano fluid coolants for advanced nuclear power plants ,Paperno.5705, in: Proceedings of ICAPP'05, Seoul,May 15 19, 2005.A.M. Rashadetal./Computers and Mathematics with Applications 62 (2011) 3140–3151 3151
13. K Khanafer, K. Vafai, M. Light stone, Buoyancy-driven heat transfer enhancement in a two dimensional enclosure utilizing a nonfluids, Int.J.Heat Mass Transfer 46(2003) 3639–3653.
14. J .Buongiorno ,Convective transport in nanofluids, ASME J.Heat Transfer 128 (2006) 240–250.
15. H. F. Oztop ,E. Abu-Nada, Numerical study of natural convection in partially heated rectangular enclosures filled with nano fluids, Int.J.Heat Fluid Flow 29 (2008)1326–1336.
16. D.A. Nield, A.V. Kuznetsov, The Cheng- Minkowycz problem for natural convective boundary laye rflow in a porous medium saturated by a nanofluid, Int. J. Heat Mass Transfer 52 (2009) 5792–5795.
17. A.V. Kuznetsov, D. A. Nield, Natural convective boundary-layer flow of a287 nanofluid past a vertical plate, Int. J. Thermal Sci.49 (2010) 243–247.
18. Syakila Ahmed, I. Pop, Mixed convection boundary layer flow from a vertical flat plate embedded in a porous medium filled with nanofluids, Int. CommonHealth Mass Transfer 37(2010) 987–991.
19. A. J. Chamkha, R. S. R. Gorla, K. Ghodeswar, Non-similar solution for natural convective boundary layer flow over a sphere embeddedin a Porous medium saturated with a nanofluid,Transp. Porous Media (2010).
20. R.S.R. Gorla, S.M. M. EL Kabeir, A. M. Rashad, Heat transfer in the boundary layer on a stretching circular cylinder in a nanofluid, J. Thermophys. Heat Transfer 25 (1) (2011)183–186.
21. R.S.R. Gorla, AliJ. Chamkha, A.M. Rashad, Mixed convective boundary layer flow over a vertical wedge embedded in a Porous medium saturated with a nano fluid, J. Nanoscale Res.Lett.6 (207) (2011) 1–9.
22. A. J. Chamkha, A.M. Aly, H. Al-Mudhaf, Laminar MHD mixed convection flow of a nanofluid along a stretching permeable surface in the presence of heat generation or absorption effects, Int.J. Microscale Nano scale Thermal Fluid Transport Phenomena 2 (2011) (Article 3).
23. A. J. Chamkha, S. Abbasbandy, A. M. Rashad, K. Vajravelu, Radiation effects on mixed convection over a wedge embedded in a Porous medium filled with a nanofluid, Transp. Porous Media (inpress).
24. A. J. Chamkha, A. M. Rashad, Natural convection from a vertical permeable cone in nano fluid saturated porous media for uniform heat and nano particles volume fraction fluxes ,Int. J. Numer. Methods Heat Fluid Flow (inpress).
25. R. H. Christopher ,S. Middleman, Power-law flow through a packed tube, I & EC Fundamentals, vol.4,1965 ,pp. 422–426.
26. R. V. Dharmadhikari, D .D. Kale, Flow of non-Newtonian fluids through porous media ,Chem. Eng. Sci .40 (1985) 527–529.
27. F. G. Blottner, Finite- difference methods of solution of the boundary- layer equations, AIAAJ. 8 (1970) 193–205.